Hyperpolarization-activated calcium channels at the tip of *Arabidopsis* root hairs

Anne-Aliénor Véry* and Julia M. Davies

Department of Plant Sciences, University of Cambridge, Downing Street, Cambridge CB2 3EA, United Kingdom

Communicated by Winslow R. Briggs, Carnegie Institution of Washington, Stanford, CA, May 31, 2000 (received for review January 16, 2000)

The root hair elongative growth phase (''tip growth''), like that of other tip-growing systems such as pollen tubes, algal rhizoids, and fungal hyphae, is associated with an apex-high cytosolic free calcium ($[Ca^{2+}]_c$) gradient generated by a local Ca^{2+} influx at the tip. This gradient has been shown to be a fundamental regulator of tip growth. Here, we have performed patch-clamp experiments at root hair apices of *Arabidopsis thaliana* (after localized cell wall laser ablation) to characterize the plasma membrane Ca^{2+} channels implicated in the tip Ca^{2+} influx. We have identified a hyperpolarization-activated Ca^{2+} conductance. This conductance is selective for Ca^{2+} over K^+ and Cl^- ($P_{Ca}/P_K = 15$; $P_{Ca}/P_{Cl} = 25$) and is fully blocked by <100-μM trivalent cations (La^{3+}, Al^{3+}, Gd^{3+}). The selectivity sequence among divalent cations (determined by comparisons of the channel unitary conductance) is $Ba^{2+} > Ca^{2+}$ (22 pS in 10 mM) $\approx Mg^{2+} > Mn^{2+}$. This conductance was operative at typical growing hair apical resting membrane potentials. Moreover, it was seen to be down-regulated in growing hair subapical regions, as well as at the tip of mature hairs (known not to exhibit Ca^{2+} influx). We therefore propose that this inward-rectifying Ca^{2+} conductance is inherently involved in the apical Ca^{2+} influx of growing hairs. The observed enhancement of the conductance by increased $[Ca^{2+}]_c$ may form part of a positive feedback system for continued apical Ca^{2+} influx during tip growth.

Root epidermal cells can differentiate to form hair-like projections that increase surface area for water and nutrient uptake, help anchor the plant, and are a key site for microbial interactions (1). Root hair development currently is divided into three stages: cell fate determination, hair initiation, and hair elongation (2). Hair elongation is extremely polarized, concerning only a narrow zone (<10 μm) at the tip, where new membrane and cell wall are built from fusion of secretory vesicles. The phenomenology of the process has been subject to intensive studies in the last 10 years, the role of Ca^{2+} ions in regulating growth being one of the main areas of research. It has been demonstrated that growth in root hairs and other tip-growing systems (e.g., pollen tubes, fucoid algal zygotes, fungal hyphae) is strongly linked to the presence of elevated apical cytosolic Ca^{2+} activity, which probably has a determinant role in the regulation of vesicle fusion (2–4). Moreover, Ca^{2+} flux studies (using Ca^{2+}-selective microelectrodes) showed that a polarized Ca^{2+} influx at the root hair tip is a prerequisite of this apical Ca^{2+} gradient (5). Although flux and imaging experiments have provided much information on the creation and regulation of apical Ca^{2+} gradients and their relation with growth, many questions remain because the transport systems responsible for Ca^{2+} entry at the root hair apex (or any other nonanimal polar growth system) have not been characterized.

Our aim was to identify and characterize such Ca^{2+} transport systems. Previous Ca^{2+} apical influx studies indicate that plasma membrane Ca^{2+}-permeable channels are the most likely candidates, and their activity is known from such studies to be restricted to the tip (5). Electrophysiological studies already have identified a number of plasma membrane transport systems in root hairs [e.g., K^+ and Cl^- channels (6–8), H^+ and Ca^{2+} ATPases (9, 10), a H^+/Cl^- symport (11)]; their spatial distribution, however, remains unknown. Critically, no root hair Ca^{2+} channel has been identified. Several kinds of Ca^{2+}-permeable channels, however, already have been identified in differentiated plant tissues, mainly in root (12). All of those, however, have been observed to have their activation domain restricted to voltages more positive than that observed across the apical plasma membrane of growing root hairs. Therefore, it is very unlikely that such channels, if present in root hairs, would be involved in continuous apical Ca^{2+} influx. To identify Ca^{2+} channels implicated in hair apical Ca^{2+} influx, we have performed local patch-clamp electrophysiology on apical plasma membrane after laser ablation of the tip cell wall (13, 14).

Here, we have discovered a hyperpolarization-activated Ca^{2+} channel, the properties of which are consistent with its being the main transport system responsible for root hair *in situ* Ca^{2+} influx. Although the channel was found to be very active at the apex of (previously) growing root hairs, it was down-regulated in regions known to exhibit no Ca^{2+} influx *in vivo* (mature hair apices and subapical regions of previously growing hairs). Moreover, channel selectivity, pharmacology, activity level, and activity domain followed the expectations obtained from previous *in vivo* flux and imaging studies.

Materials and Methods

Root Hair Growth and Membrane Recovery. Seedlings were grown aseptically for 3 days from surface-sterilized seeds (2) of *Arabidopsis thaliana* (ecotype Columbia) at 22°C on 0.1 mM KCl and 0.1 mM $CaCl_2$ (pH 5.6) solidified with 1% (wt/vol) agar. After seedling transfer to the patch-clamp chamber, hair growth rates were determined in a solution of the same salt composition before further experimentation. Laser microsurgery, for apical membrane recovery, was adapted from previously described protocols (13, 14). Rapid hair-tip plasmolysis (2–3 min) was achieved by 350 mM mannitol (with 5 mM $CaCl_2$). In addition to the retraction of the membrane from the cell wall at the tip, the hyperosmotic solution often led to a fragmentation of the hair protoplast (producing a succession of hair ''spheroplasts''). Laser cell-wall cutting of a few hairs ($\approx$5 min) was performed at their tip. The release of the apical portion of the hair protoplast (first ''spheroplast'' or apical part of it) was achieved by deplasmolysis (1–2 min), the osmolarity being reduced to 275 mOsM (2.5 mM $CaCl_2$). Such apical spheroplasts were, in agreement with hair morphology (2), very densely cytoplasmic when isolated from previously fast-growing hairs ($\approx$1 $\mu m \cdot min^{-1}$) and vacuolated when isolated from previously slow-growing hairs (<0.2 $\mu m \cdot min^{-1}$). They were excised by gently shaking the chamber. In some experiments, we were interested in recovering

Abbreviations: $[Ca^{2+}]_c$, free cytosolic Ca^{2+}; *I–V*, current–voltage.

*To whom reprint requests should be sent at the present address: Laboratoire de Biochimie et Physiologie Moléculaire des Plantes, UMR 5004 AgroM/Centre National de la Recherche Scientifique/Institut National de la Recherche Agronomique/Université Montpellier, Campus AgroM-Institut National de la Recherche Agronomique, Place Viala, 34060 Montpellier Cedex 1, France. E-mail: very@ensam.inra.fr.

The publication costs of this article were defrayed in part by page charge payment. This article must therefore be hereby marked "*advertisement*" in accordance with 18 U.S.C. §1734 solely to indicate this fact.

Article published online before print: *Proc. Natl. Acad. Sci. USA*, 10.1073/pnas.160250397. Article and publication date are at www.pnas.org/cgi/doi/10.1073/pnas.160250397

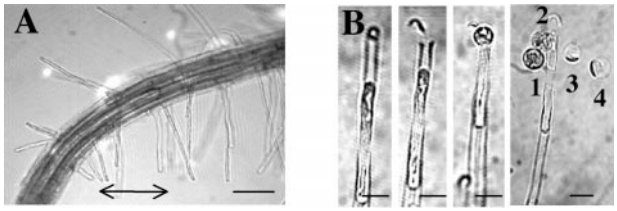

Fig. 1. Recovery of plasma membrane at the apex and subapical region of young root hairs. (*A*) Apex of a 3-day-old *A. thaliana* root. The arrow marks young, growing hairs used for experiments. (Bar = 100 μm.) (*B*) *In situ* laser microsurgery and recovery of hair spheroplasts (12, 13). (From left to right) Root hair tip plasmolysis; tip cell wall cut by laser; recovery of apical plasma membrane by hair deplasmolysis; recovery of subapical plasma membrane by stronger deplasmolysis. Numbers mark the order of spheroplast extrusion from the tip. (Bar = 15 μm.)

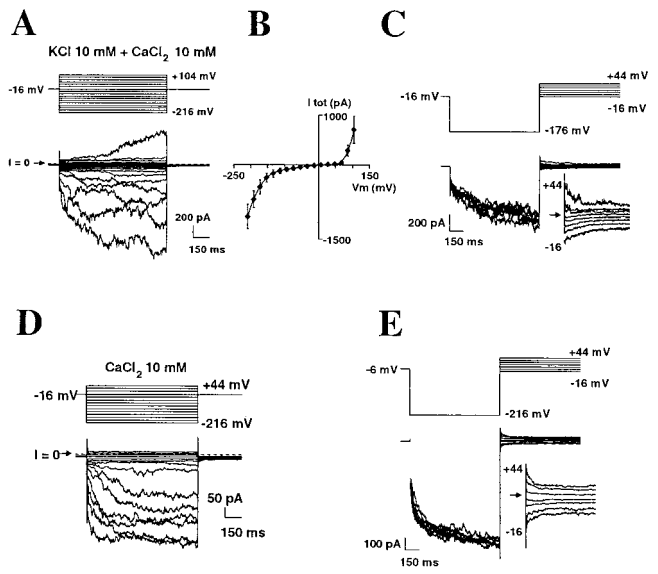

Fig. 2. Hyperpolarization-activated calcium currents at the tip of growing root hairs. (*A*–*E*) Whole-cell patch-clamp, with voltage-clamp protocol shown above current traces. (*A*–*C*) K^+-containing solutions. Free internal Ca^{2+} concentration was 520 nM. (*B*) Mean (±SEM) *I–V* curve of total current ($n = 6$). (*C*) Evidence for a Ca^{2+} component in the inward current by tail current analysis; the arrow marks current reversal. (*D* and *E*) Extraction of the Ca^{2+} component. Similar experiments to *A* and *C*, but with KCl and K-glutamate removed from solutions.

membrane from subapical regions of previously fast-growing hairs. Subapical spheroplasts were recovered by reducing further the bath osmolarity (200 mOsM, 2.5 mM $CaCl_2$). A succession of hair spheroplasts then was released. Highly vacuolated subapical spheroplasts were chosen (i.e., originating from the region occupied by a large central vacuole; e.g., third and fourth spheroplasts released in Fig. 1) to ensure that no confusion could be made with the apical spheroplast.

Batches of spheroplasts were renewed every 1.5–2 h as seal formation became very difficult and the Ca^{2+} conductance in the spheroplasts started to decline after this time period.

Patch-Clamp Solutions. All patch-clamp solutions were adjusted to 275 mOsM with mannitol. The basal external (bath) solution comprised 10 mM $CaCl_2$ and 5 mM Mes/Tris, pH 6.0, unless stated otherwise. K^+, when present, was added as 10 mM KCl. In K^+-free solutions, other divalent cations (as chloride salts) sometimes replaced Ca^{2+} as indicated in the figure legends. In channel-blocker experiments, trivalent cations were added as chloride salts. In experiments with $AlCl_3$, pH was reduced to 4.5 for both control and test solutions. Unless otherwise stated, the basal internal (pipette) medium comprised 0.5 mM $CaCl_2$, 4 mM $Ca(OH)_2$, 2 mM MgATP, 0.5 mM Tris ATP, 10 mM 1,2-bis(2-aminophenoxy)ethane-*N,N,N′,N′*-tetraacetic acid, 15 mM Hepes/Tris, pH 7.3; free Ca^{2+} was 100 nM. Other values of free Ca^{2+} were obtained by varying $Ca(OH)_2$. Free [Ca^{2+}] was estimated with the program MAXCHELATOR (15). It should be noted that free cytosolic Mg^{2+} was around 600 μM (i.e., always more than 100 times greater than free Ca^{2+}). It therefore is unlikely that significant changes in surface charge potential may have occurred when free Ca^{2+} was varied. Potassium sometimes was included as 100 mM K-glutamate (Fig. 2 *A–C*). In experiments in which selectivity among divalent cations was examined (Fig. 3), 20 mM EGTA replaced 1,2-bis(2-aminophenoxy)ethane-*N,N,N′,N′*-tetraacetic acid to avoid accumulation of the other divalent cations at the cytoplasmic side.

Patch-Clamp Recording. Classical patch-clamp methods were used (14). Data were sampled at 1 kHz and filtered at 200 Hz. Membrane potentials were corrected for liquid junction potentials and series resistance. Two types of voltage-clamp protocols were used for investigation of the membrane conductance. (*i*) The first was a series of depolarizing and/or hyperpolarizing steps of 1-s duration from a holding potential, unless stated otherwise, in the range +10 to −30 mV (i.e., close to the resting potential of the spheroplasts in the patch-clamping solutions). Current–voltage relationships (*I–V* curves) then were constructed with total whole-cell currents measured after 1 s of voltage clamp. (*ii*) Alternatively, the membrane conductance was investigated by performing slow ramps of potential (10–30 mV/s) after a 1-s holding pulse in the range of −180 to −200 mV. This second protocol enabled a faster scan of the conductance over the −200 to +100 mV domain and often was preferred in selectivity and block experiments to minimize risks of drift of the current level.

Total currents were recorded at least 10 min after attainment of the whole-cell mode to ensure that equilibration of the pipette solution with the cytoplasm was as complete as possible. Hyperpolarization-activated Ca^{2+} currents generally were stable after this time period, when free Ca^{2+} in the pipette solution was <150 nM (i.e., close to the probable resting free Ca^{2+} of our spheroplasts, the plasmolysis step necessary for spheroplast isolation very likely having dissipated the hair tip-localized high cytosolic Ca^{2+}). However, when higher free Ca^{2+} was used in the pipette solution, we observed that 30–50 min often were necessary for Ca^{2+} current stabilization. In experiments in which the effect of free Ca^{2+} on Ca^{2+} currents was investigated, currents therefore were systematically monitored for up to 50 min, and values presented in the manuscript are mean values of currents recorded at 30, 40, and 50 min after whole-cell attainment.

Results

Identification of a Ca^{2+}-Selective, Inward-Rectifying Conductance at the Apex of Young Root Hairs. Root hair apical plasma membrane was recovered from 3-day-old seedlings of *A. thaliana* (Fig. 1). We first focused our investigation on young, growing hairs 80–150 μm long with a growth rate of approximately 1 μm·min^{-1}, located close to the root apex. We checked that such root hairs could restart growth after exposure to the plasmolysis/deplasmolysis regime (without laser cutting); 57% of hairs restarted growth within 30 min of the return to control conditions ($n = 7$). The growth rate recovery was 48%; mean (±SEM) control growth rate, 0.93 ± 0.13 μm·min^{-1}; recovery growth rate, 0.45 ± 0.13 μ·min^{-1} ($n = 4$). Apical spheroplasts obtained from young hairs were very densely cytoplasmic (diameter, ≈15 μm).

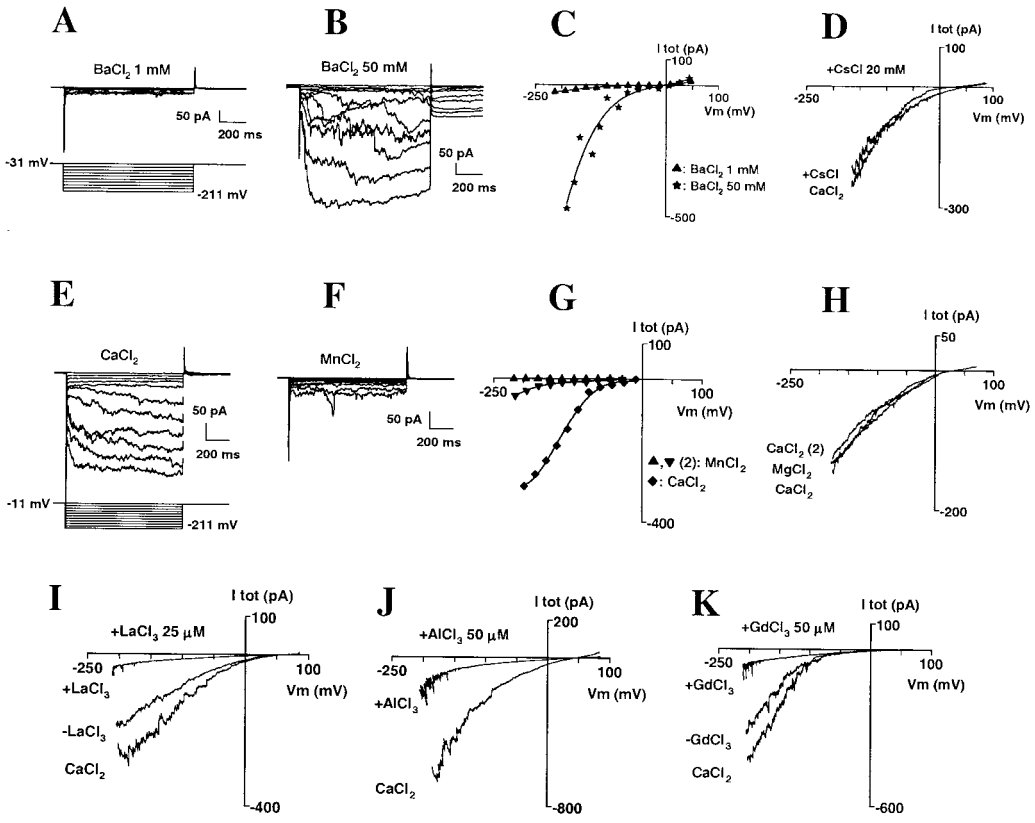

Fig. 3. Selectivity and block of the inward Ca^{2+} current. (*A–C*) Whole-cell current sensitivity to increases in external $BaCl_2$ concentration; successively 1 (*A*) and 50 (*B*) mM. (*C*) Corresponding *I–V* curve of total current. (*D*) Effect of the addition of CsCl (20 mM) on Ca^{2+} current. External $CaCl_2$ was 10 mM; traces were obtained by hyperpolarizing the membrane to −200 mV during 1 s to activate the Ca^{2+} conductance, then slowly depolarizing (30 mV/s) up to +90 mV; each trace is the average of three successive repeats. Currents were plotted against corresponding voltages. (*E–G*) Comparison of whole-cell currents with external Ca^{2+} or Mn^{2+}. Currents were recorded successively in 10 mM $MnCl_2$ (traces not shown), $CaCl_2$ (*E*), and, again, $MnCl_2$ (*F*). (*G*) Corresponding *I–V*. (*H*) Comparison of whole-cell currents with external Ca^{2+} or Mg^{2+}. Currents were recorded successively in 10 mM $CaCl_2$, $MgCl_2$, and, again, $CaCl_2$; voltage-clamp protocol was similar to that in *D*. (*I–K*) Block of the Ca^{2+} current by La^{3+} (*I*; 25 μM), Al^{3+} (*J*; 50 μM), and Gd^{3+} (*K*; 50 μM). External $CaCl_2$ was 10 mM; Voltage-clamp protocols were similar to *D*.

Whole-cell recordings from these spheroplasts in K^+-based media containing 10 mM external $CaCl_2$ showed a large, time-dependent, inward-rectifying conductance at hyperpolarized potentials (more negative than around −100 mV) and an outward-rectifying conductance when the membrane was depolarized beyond +80 mV (Fig. 2 *A–C*). The reversal potential of the inward current (Fig. 2*C*) ranged from −6 to + 24 mV (mean ± SEM: +6 ± 5.5 mV, $n = 5$). This was clearly positive to the equilibrium potentials of both K^+ ($E_K = -56$ mV) and Cl^- ($E_{Cl} = -88$ mV), which suggested the presence of a Ca^{2+} component ($E_{Ca} = +129$ mV) in this inward current. The outward-rectifying current was carried mainly by K^+ in these conditions (not shown).

To analyze further the Ca^{2+} component of the inward conductance, K^+ was removed from all solutions. Inward-rectifying currents still were observed (Fig. 2*D*). They were found in all spheroplasts investigated ($n = 18$ for the K^+-free conditions specific to Fig. 2*D*; $n > 100$ for the entire study) and reversed at +27 ± 4 mV (Fig. 2*E*; tail current analysis performed on six of the 18 trials). This indicates a permeability ratio of P_{Ca}/P_{Cl} of 25 [calculated from Goldman equation (16): $I_{Ca} + I_{Cl} = 0$, with the hypothesis that $P_{Mg} = P_{Ca}$, see below]. Using this value of P_{Ca}/P_{Cl}, $P_{Ca}/P_K = 15$ could be deduced from experiments described above with both K^+ and Ca^{2+} in the media.

Inward currents also were observed when $BaCl_2$ replaced external $CaCl_2$. Increasing $BaCl_2$ from 1 to 50 mM (Fig. 3 *A–C*; $n = 3$) strongly increased the inward current, which confirmed its mainly cationic nature and demonstrated that this Ca^{2+} conductance does not involve the classical K^+ inward rectifier (6, 17), which is blocked by barium (18). This also was confirmed by the observation that the Ca^{2+} current was not blocked by the addition of 12 mM Cs^+ (another blocker of the K^+ inward rectifier; refs. 6 and 19) to the bath (Fig. 3*D*; $n = 3$). Therefore, it can be concluded that we were observing a Ca^{2+}-selective, inward-rectifying conductance.

Currents that were approximately 10 times smaller were recorded after exchanging equimolar external $CaCl_2$ for $MnCl_2$ (Fig. 3 *E–G*; $n = 8$). Currents of comparable size were recorded in $CaCl_2$ and $MgCl_2$ (Fig. 3*H*; $n = 3$). Experiments with channel blockers showed the Ca^{2+} conductance was strongly inhibited by La^{3+}, Al^{3+}, and Gd^{3+} (Fig. 3 *I–K*). In the presence of 10 mM external Ca^{2+} and 20 μM La^{3+}, 30 μM Al^{3+}, or 30 μM Gd^{3+}, the current inhibition at −170 mV was, respectively, 85 ± 3% ($n = 5$), 70 ± 7% ($n = 5$), and 75 ± 8% ($n = 4$). Nifedipine (100 μM) was much less effective (17 ± 9% inhibition, $n = 3$; not shown).

At the single-channel level, we identified a hyperpolarization-activated, Ca^{2+}-selective channel (Fig. 4 *A–E*). The conductance in 10 mM external $CaCl_2$ was 22 pS (Fig. 4*F*; $n = 6$). The channel's P_{Ca}/P_{Cl} ratio deduced from current reversal potential (Fig. 4*F*) equaled that of the whole-cell inward current. The channel conductance was 40, 20, and 7 pS when, respectively, 10 mM Ba^{2+}, Mg^{2+}, and Mn^{2+} replaced Ca^{2+} in the external medium (Fig. 4 *A* and *C–F*). When Mn^{2+} replaced Ca^{2+}, a strong but reversible reduction of the channel activity accompanied the

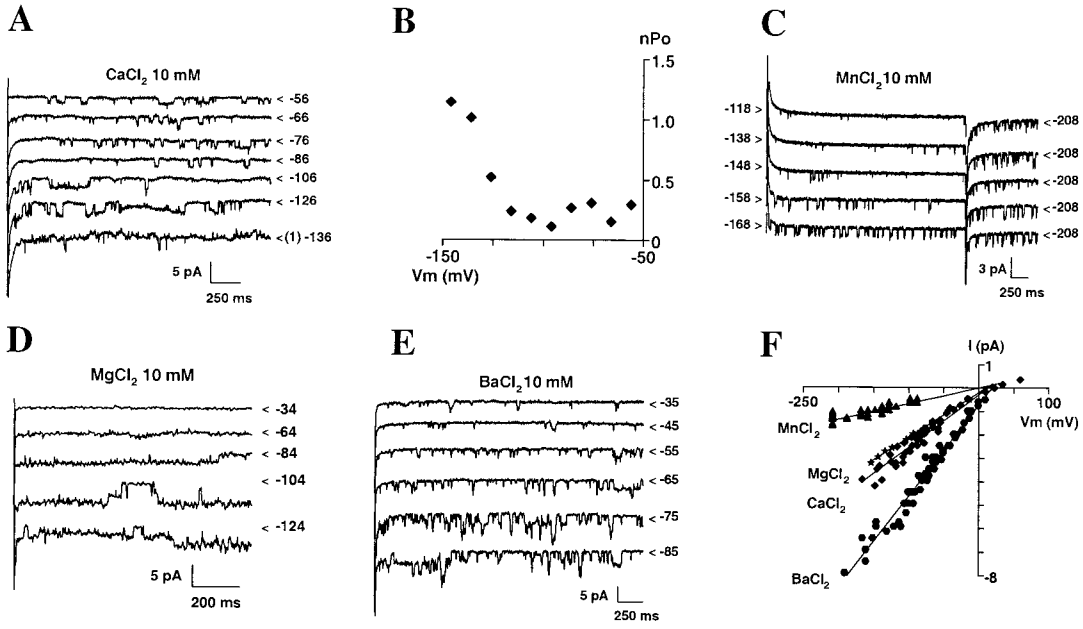

Fig. 4. Single-channel features of the inward-rectifying Ca^{2+} channel. (*A* and *B*) Examples of traces (*A*) and analysis of channel activation (*B*, same patch) from an outside-out patch bathed in 10 mM $CaCl_2$. Cl^- and Ca^{2+} equilibrium potentials were −77 and +150 mV (E_{Ca+Mg} = +40 mV), respectively. (*A*) < indicates the lowest level of current; it corresponds to zero channel open except at −136 mV, where baseline corresponds to one channel open (1). The membrane potential is indicated to the right of each trace. Holding potential was −56 mV. (*B*) nPo (n, number of active channels; Po, open probability) was extracted from 3-s pulses. (*C–E*) Examples of single-channel traces in 10 mM of either $MnCl_2$ (*C*; same patch as in *A*), $MgCl_2$ (*D*), or $BaCl_2$ (*E*). Holding potential was −208 mV in *C*, because channel activity had strongly declined in $MnCl_2$, −14 mV in *D*, and +5 mV in *E*. (*F*) Single-channel *I–V* relationships with 10 mM external concentration of either Ca^{2+}, Mn^{2+}, Mg^{2+}, or Ba^{2+}. Ten experiments have been pooled.

conductance decrease (Fig. 4 *A* and *C*), which is in agreement with the observation of stronger current reduction at the whole-cell level. The similar activation and selectivity properties at the single-channel and whole-cell level, plus the fact that no other inward-rectifying, Ca^{2+}-permeable channel was observed (n = 28), suggest that this channel very likely is the main component of the whole-cell Ca^{2+} conductance.

Regulation of the Ca^{2+} Currents by Cytosolic Ca^{2+}. Free cytosolic Ca^{2+} ($[Ca^{2+}]_c$) at the tip fluctuates with growth (2). Values range from around 150 nM in nongrowing hairs exhibiting no net Ca^{2+} influx to up to 1.6 μM in fast-growing ones. Dynamic Ca^{2+} influx (already demonstrated in pollen tubes; ref. 20) is expected. We examined whether $[Ca^{2+}]_c$ could regulate our Ca^{2+} conductance (Fig. 5*A*). Whole-cell Ba^{2+} currents were compared in the presence of either 10, 100, or 900 nM $[Ca^{2+}]_c$. Varying $[Ca^{2+}]_c$ in the physiological range (100 to 900 nM) modulated the Ca^{2+} conductance, with higher $[Ca^{2+}]_c$ shifting its activation toward less negative membrane potentials (40-mV shift). Below 100 nM, the same phenomenon was observed, although to a lesser extent. Thus, *in vivo*, elevated $[Ca^{2+}]_c$ (by net influx or store release) could induce further Ca^{2+} influx through this conductance, a property that could be important to pulsatile growth (2) and trajectory change (when strong Ca^{2+} influx must be reinitiated; refs. 21 and 22).

Varying free cytosolic Mg^{2+} from 600 to 15 μM did not evoke any deactivation of current (not shown), suggesting that the effects of cytosolic Ca^{2+} may be specific.

Spatial and Temporal Differences in Ca^{2+} Currents. After a few hours of elongation, root hair growth declines and eventually stops. Maturation is accompanied by increased vacuolation, loss of the densely cytoplasmic zone at the tip, loss of tip Ca^{2+} influx (5), and the cytoplasmic gradient (2). We examined whether apical spheroplasts from mature hairs had different Ca^{2+} current patterns from those from younger, growing hairs (Fig. 5 *B–E*). Apical spheroplasts from slowly growing older hairs (rate < 0.2 $\mu m \cdot min^{-1}$) examined in the presence of 100 nM $[Ca^{2+}]_c$ (which approximates the $[Ca^{2+}]_c$ of such hairs; refs. 2 and 23) exhibited the inward Ca^{2+} conductance (Fig. 5*C*). It activated, however, at far more hyperpolarized potentials than in spheroplasts from juvenile hairs (Fig. 5*B*) in the same conditions (shift of approximately 60–80 mV, Fig. 5*E*). Single-channel experiments carried out on spheroplasts from mature tips confirmed that the conductance was the same as that found in spheroplasts from young, growing hairs (not shown). Because growing hairs have higher $[Ca^{2+}]_c$ at their tip (0.5–1.6 μM; refs. 2 and 23) than mature ones, the difference in activation properties between nongrowing and fast-growing tips is likely to be even more pronounced (approximately 100–120 mV; see Fig. 5*A*). This difference probably explains why, at resting potential, Ca^{2+} influxes occur in growing hairs but not in nongrowing ones (5).

In growing hairs, only the tip is engaged in net Ca^{2+} influx (5). The presence of the Ca^{2+} inward conductance therefore also was examined in plasma membrane from subapical regions of hairs that were growing before experimentation (Fig. 5*D*). Currents recorded in subapical regions were very similar to those recorded at the tip of the older, "nongrowing" hairs; i.e., the Ca^{2+} conductance was present but its apparent activation domain shifted to voltages more negative than the resting membrane potentials measured subapically (9). Although it was not technically possible to assay apical and subapical spheroplasts from the same hair, because both types were subject to the same recording protocols (solutions, time elapsed after release, etc.), it is unlikely that the differences between the two populations are artifactual.

Discussion

We describe here a hyperpolarization-activated, Ca^{2+}-selective conductance in root hairs of *A. thaliana*. To date, plant hyper-

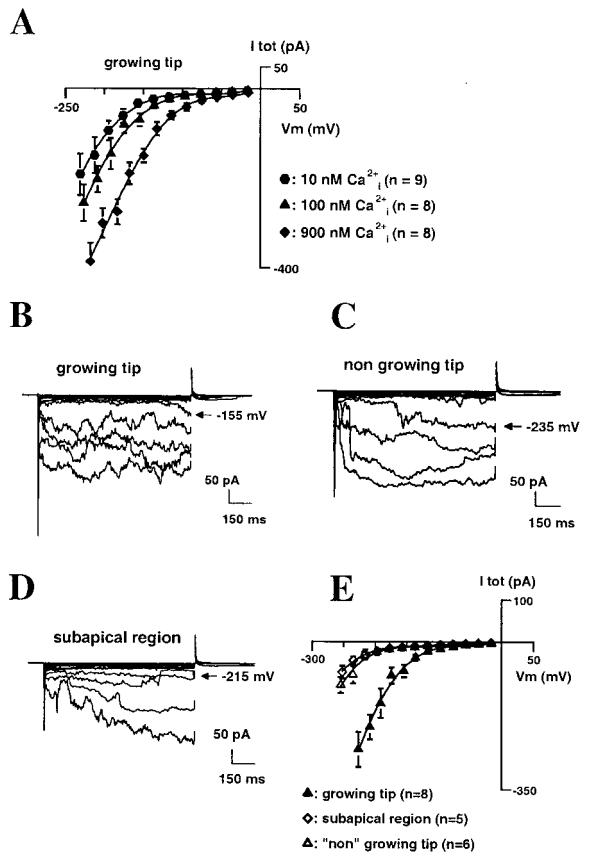

Fig. 5. Regulation of the inward Ca^{2+} current. (*A*) Effect of internal Ca^{2+} concentration on Ca^{2+} currents at the tip of young hairs. Whole-cell currents were recorded in the presence of 10 mM external $BaCl_2$ and 10, 100, or 900 nM internal free Ca^{2+} [free Ca^{2+} controlled with 1,2-bis(2-aminophenoxy)ethane-*N*,*N*,*N*′,*N*′-tetraacetate]. Three successive recordings were performed 30, 40, and 50 min after whole-cell attainment and averaged for each spheroplast examined. (*B–E*) Comparison of Ca^{2+} currents in growing and nongrowing regions. Typical example of current traces in spheroplasts from the tip of a young hair (growth rate $\cong$ 1 $\mu m \cdot min^{-1}$) (*B*), from the tip of a ''nongrowing'' hair (growth $<$ 0.2 $\mu m \cdot min^{-1}$) (*C*), and from subapical regions (*D*). Currents were recorded in the presence of 10 mM external $BaCl_2$ and 100 nM internal free Ca^{2+}. (*E*) Mean $\pm$ SEM *I–V* relationships for the three regions. Recordings from mature hairs and subapical regions were obtained in the same conditions as those from tips of young hairs (similar time after spheroplast release, same time after whole-cell attainment).

polarization-activated plasma membrane calcium currents have been characterized only in undifferentiated suspension culture cells (24, 25). The root hair and culture cell channels share several properties: comparable P_{Ca}/P_K and P_{Ca}/P_{Cl} values, sensitivity to La^{3+} and nifedipine, and higher conductance in $BaCl_2$ than in $CaCl_2$. The conductance of the root hair channel in $CaCl_2$ or $BaCl_2$, however, is 5–10 times greater, which suggests a different identity. Ca^{2+} conductances active at hyperpolarized potentials have been described in animal cells. They mainly include several types of store-operated channels (26) and a few other receptor-activated conductances (26, 27). That the activity of the root hair Ca^{2+} conductance is reduced (Fig. 5*A*) in low Ca^{2+} and high 1,2-bis(2-aminophenoxy)ethane-*N*,*N*,*N*′,*N*′-tetraacetate conditions (which are likely to induce internal store depletion) and increased by high cytosolic Ca^{2+} suggests that this conductance is not likely to be a store-operated channel homologous to those described in animal cells (27, 28), although further experimentation would be necessary to dismiss this hypothesis irrefutably.

Three main lines of evidence support the inherent involvement of the hyperpolarization-activated Ca^{2+} conductance in root hair apical Ca^{2+} fluxes: (*i*) voltage and cytosolic Ca^{2+} activation, (*ii*) temporal and spatial activity, and (*iii*) selectivity and pharmacological profile. First, the conductance is strongly active at resting membrane potentials and apical $[Ca^{2+}]_c$ typical of growing root hairs. *Arabidopsis* root hairs growing, as in this study, at a rate of close to 1 $\mu m \cdot min^{-1}$ (and in a similar medium) have been shown to have subapical resting potentials in the range of -160 to -200 mV (9). A local depolarization at the extreme apex is expected because of the occurrence of a net apical inward current. This apical depolarization, however, seems to be of very small amplitude (e.g., 5 mV; ref. 23). The Ca^{2+} conductance that we identified was seen to be active in young hair tip spheroplasts at physiological $[Ca^{2+}]_c$ of growing tips (0.5–1.6 μM; refs. 2 and 23) at membrane voltages more negative than at least -120 mV. This conductance, therefore, is very likely to be active at growing hair tip resting potentials. At this point, we cannot discount the existence of depolarization-activated Ca^{2+} channels in the root hair plasma membrane because the recording conditions used here may not favor their activity (e.g., quite a long solution equilibration time after whole-cell attainment before recording; see ref. 29). However, the depolarization-activated Ca^{2+} channels identified so far in root tissue (12) are not active at potentials more negative than -140 mV, which suggests that their involvement in continuous uptake at the root hair apex is not feasible.

Furthermore, the amplitude of the macroscopic hyperpolarization-activated Ca^{2+} current in apical spheroplasts from growing root hairs is in agreement with fluxes measured *in vivo.* Net Ca^{2+} influx measured at the apex of growing *Arabidopsis* root hairs in the presence of 100 μM external Ca^{2+} is around 3–5 $pmol \cdot cm^{-2} \cdot s^{-1}$ (5). This would correspond in a tip spheroplast of 15-μm diameter to an inward current of 1–2.5 pA and, in our recording conditions (10 mM Ba^{2+}), to up to 200–500 pA [assuming no saturation of current (30) and a conductance ratio, Ba^{2+}/Ca^{2+}, of 2; Fig. 4*F*]. This is in the range of what was recorded here from tip spheroplasts (Fig. 5*A*).

In agreement with the lack of Ca^{2+} influx at subapical regions of growing hairs and at the tip of mature nongrowing hairs (5), the hyperpolarization-activated Ca^{2+} conductance was seen to be down-regulated in these two regions. We were aware that it was feasible that although spheroplast isolation was rapid (10–15 min), the plasmolysis/deplasmolysis treatment might have modified the distribution of plasma membrane transport systems. That clear differences were observed between apical and subapical regions and young and mature apices strongly suggests that inherent polarities in Ca^{2+} channel activity remained. In nongrowing regions, the apparent activation voltage of the Ca^{2+} conductance shifted negative to that found at the apex of young root hairs. Hence, *in vivo* at resting membrane potential, Ca^{2+} influx would be prevented. At present, the mechanism of this down-regulation can only be speculated on. It has been shown in growing pollen tubes that some messengers and regulatory proteins [e.g., phosphatidylinositol 4,5-biphosphate (31), GTPases (31, 32), kinases (33)] have a polarized distribution, with a greater concentration in growing tips. Temporal and spatial differences in the activity of the Ca^{2+} conductance may well rely on fine regulation (e.g., difference in protein association, phosphorylation status) generated by the local cytoplasmic environment.

The selectivity and pharmacological profile of the identified Ca^{2+} conductance is in agreement with what is known so far of the Ca^{2+} conductance responsible for root hair apical Ca^{2+} influx. Indeed, previous *in situ* flux and imaging studies have revealed a permeability comparable to Ca^{2+} and Mg^{2+} (34), at least a slight permeability to Mn^{2+} (2), and a stronger sensitivity to trivalent cations [La^{3+} (23); Al^{3+} (34)] than to nifedipine (5, 30). These properties are shared by our Ca^{2+} conductance. The

weak blockage by 100 μM nifedipine in our experiments may look at first sight inconsistent with the greater levels of growth inhibition reported in *in situ* studies. It may be explained, however, by a Ca^{2+} dependence of the dihydropyridine potency, as is the case in animal L-type Ca^{2+} channels (16, 35), the present study having been carried out with 100 times greater external Ca^{2+} than that used previously.

Overall, the characteristics of the hyperpolarization-activated Ca^{2+} conductance are consistent with previous data from root hair studies, which point to a key role in apical influx. Because no other Ca^{2+}-permeable channels active at typical hair resting potentials were detected here, it is possible that this conductance is the sole entry route for Ca^{2+}. However, it must be recognized that any patch-clamp preparative procedure (laser or enzymatic) risks channel ''loss'' by endocytosis or inactivation, and it would be premature to draw such a conclusion from the absence of other channel types. Given that caveat, does this new conductance fit into the accepted models for tip growth or should they now be restructured? The combination of imaging and flux measurement studies in growing pollen tubes has led to the proposal of two models for the establishment of apical cytosolic Ca^{2+} gradients (20). The ''internal stores'' model relies on apical stretch-activated plasma membrane channels to let Ca^{2+} in, which induces Ca^{2+} release from internal stores, the latter then being refilled by a plasma membrane store-operated Ca^{2+} channel. In the ''external stores'' model, Ca^{2+} entry is simply through apical stretch-activated plasma membrane channels, the regulation of which is linked to the cell wall. These models were proposed to account for the fact that cytosolic Ca^{2+} and Ca^{2+} fluxes often were seen to oscillate at the tip of growing pollen tubes (36) and that a delay between the two peaks of oscillations was observed (37). Although flux and cytosolic Ca^{2+} oscillations have not been described yet in root hairs, their occurrence is likely; pulsatory root hair growth rates have been reported (2). In both of these existing models, however, the proposal of the type of Ca^{2+} conductances involved was extremely speculative. No experimental result exists in favor of the presence of a store-operated conductance in any plant tip-growing system, and little evidence (weak pharmacological evidence) supports the idea that stretch-activated channels are pivotal. In contrast, the unequivocal identification here of inward-rectifying Ca^{2+} channels will enable development of a new (perhaps simpler) model with channel activity dynamically regulated by voltage and internal calcium. It is feasible that the Ca^{2+} that permeates the channel then contributes to its further activation as part of a positive feedback system to ensure continued apical influx.

In conclusion, although Ca^{2+} influx at the apices of plant tip-growing cells has been known for several years to be a key determinant in controlling tip growth, the Ca^{2+} channels that are involved had not been characterized. Here, we described a root hair channel that is likely to be responsible mainly for *in vivo* apical Ca^{2+} influx. The challenge now is to understand fully the channel's regulation at root hair initiation and maturity, as well as during pulsatory elongation.

We thank our colleagues for comments. The work was supported by Biotechnology and Biological Sciences Research Council and Natural Environment Research Council awards to J.M.D.

1. Peterson, R. L. & Farquhar, M. L. (1996) *Bot. Rev.* **62,** 1–35.
2. Wymer, C. L., Bibikova, T. N. & Gilroy, S. (1997) *Plant J.* **12,** 427–439.
3. Miller, D. D., de Ruijter, N. C. A. & Emons, A. M. C. (1997) *J. Exp. Bot.* **48,** 1881–1896.
4. Malhó, R. (1998) *Trends Plant Sci.* **3,** 40–42.
5. Schiefelbein, J. W., Shipley, A. & Rowse, P. (1992) *Planta* **187,** 455–459.
6. Gassmann, W. & Schroeder, J. I. (1994) *Plant Physiol.* **105,** 1399–1408.
7. Grabov, A. & Böttger, M. (1994) *Plant Physiol.* **105,** 927–935.
8. Bouteau, F., Pennarun, A.-M., Kurkdjian, A., Convert, M., Cornel, D., Monestiez, M., Rona, J.-P. & Bousquet, U. (1999) *Plant Physiol. Biochem.* **37,** 889–898.
9. Lew, R. R. (1996) *Plant Physiol.* **112,** 1089–1100.
10. Felle, H. H., Tretyn, A. & Wagner, G. (1992) *Planta* **188,** 306–313.
11. Felle, H. H. (1994) *Plant Physiol.* **106,** 1131–1136.
12. White, P. J. (1998) *Ann. Bot.* **81,** 173–183.
13. Kurkdjian, A., Leitz, G., Manigault, P., Harim, A. & Greulich, K. O. (1993) *J. Cell Sci.* **105,** 263–268.
14. Véry, A.-A. & Davies, J. M. (1998) *Appl. Environ. Microbiol.* **64,** 1569–1572.
15. Bers, D. M., Patton, C. W. & Nuccitelli, R. (1994) *Methods Cell Biol.* **40,** 3–29.
16. Hille, B. (1992) *Ionic Channels of Excitable Membranes* (Sinauer, Sunderland, MA), 2nd Ed.
17. Fairley-Grenot, K. A. & Assmann, S. M. (1992) *J. Membr. Biol.* **128,** 103–113.
18. Schroeder, J. I. (1987) *Proc. Natl. Acad. Sci. USA* **84,** 4108–4112.
19. Ichida, A. M., Pei, Z.-M., Baizabal-Aguirre, V. M., Turner, K. J. & Schroeder, J. I. (1997) *Plant Cell* **9,** 1843–1857.
20. Holdaway-Clarke, T. L., Feijó, J. A., Hackett, G. R., Kunkel, J. G. & Hepler, P. K. (1997) *Plant Cell* **9,** 1999–2010.
21. Bibikova, T. N., Zhigilei, A. & Gilroy, S. (1997) *Planta* **203,** 495–505.
22. Malhó, R. & Trewavas, A. J. (1996) *Plant Cell* **8,** 1935–1949.
23. Felle, H. H. & Hepler, P. K. (1997) *Plant Physiol.* **114,** 39–45.
24. Gelli, A. & Blumwald, E. (1997) *J. Membr. Biol.* **155,** 35–45.
25. Gelli, A. Higgins, V. J. & Blumwald, E. (1997) *Plant Physiol.* **113,** 269–279.
26. Parekh, A. B. & Penner, R. (1997) *Physiol. Rev.* **77,** 901–930.
27. Fasolato, C., Innocenti, B. & Pozzan, T. (1994) *Trends Pharmacol. Sci.* **15,** 77–83.
28. Berridge, M. J. (1995) *Biochem. J.* **312,** 1–11.
29. Thion, L., Mazars, C., Nacry, P., Bouchez, D., Moreau, M., Ranjeva, R. & Thuleau, P. (1998) *Plant J.* **13,** 603–610.
30. Herrmann, A. & Felle, H. H. (1994) *New Phytol.* **129,** 523–533.
31. Kost, B., Lemichez, E., Spielhofer, P., Hong, Y., Tolias, K., Carpenter, C. & Chua, N. H. (1999) *J. Cell Biol.* **145,** 317–330.
32. Lin, Y., Wang, Y., Zhu, J.-K. & Yang, Z. (1996) *Plant Cell* **8,** 293–303.
33. Moutinho, A., Trewavas, A. J. & Malhó, R. (1998) *Plant Cell* **10,** 1499–1509.
34. Jones, D. L., Shaff, J. E. & Kochian, L. V. (1995) *Planta* **197,** 672–680.
35. Lee, K. S. & Tsien, R. W. (1983) *Nature (London)* **302,** 790–794.
36. Pierson, E. S., Miller, D. D., Callaham, D. A., van Aken, J., Hackett, G. & Hepler, P. K. (1996) *Dev. Biol.* **174,** 160–173.
37. Messerli, M. & Robinson, K. R. (1997) *J. Cell. Sci.* **110,** 1269–1278.